Hypothalamic prostaglandins facilitate recovery from hypoglycemia but exacerbate recurrent hypoglycemia in mice

Takashi Abe[1#], Shucheng Xu[2#], Yuki Sugiura[3], Yuichiro Arima[4], Takahiro Hayasaka[5], Ming-Liang Lee[6], Taiga Ishimoto[1], Yudai Araki[1], Ziwei Niu[1], Norifumi Iijima[7], Sabrina Diano[8], Chitoku Toda*[1]

[1] Department of Neuroscience for Metabolic Control, Faculty of Life Sciences, Kumamoto University, Kumamoto, Japan

[2] Laboratory of Biochemistry, Graduate School of Veterinary Medicine, Hokkaido University, Hokkaido, Japan.

[3] Multiomics Platform, Center for Cancer Immunotherapy and Immunobiology, Kyoto University Graduate School of Medicine, Kyoto, Japan

[4] International Research Center for Medical Sciences (IRCMS), Kumamoto University, Kumamoto, Japan

[5] Institute for the Advancement of Higher Education, Hokkaido University, Hokkaido, Japan.

[6] Exploratory Research Center on Life and Living Systems (ExCELLS), National Institutes of Natural Sciences (NINS), Aichi, Japan

[7] National Institutes of Biomedical Innovation, Health and Nutrition, Osaka, Japan

[8] Institute of Human Nutrition, Columbia University Irving Medical Center, New York, United States

[#] These authors equally contributed to this work

* Corresponding author: toda-c@kumamoto-u.ac.jp

Abstract

The hypothalamus regulates systemic glucose metabolism by monitoring glucose levels. In response to hypoglycemia, glucose-inhibited (GI) neurons promote counter-regulatory responses (CRRs) stimulating glucagon, epinephrine, and cortisol secretions. Recurrent hypoglycemia (RH) attenuates CRRs. Here, we show that prostaglandins are produced in the hypothalamus during hypoglycemia to activate GI neurons and thus increase glucagon secretion. RH attenuated glucose production by decreasing glucagon secretion. RH caused a metabolic adaptation and preserved

intermediates of glycolysis and amino acids in the hypothalamus during hypoglycemia. Inhibition of prostaglandin production by using short-hairpin RNA (shRNA) against cytosolic phospholipase A2 (cPLA2) in the hypothalamus decreased the attenuation of CRRs by RH. CRR hormones and the activity of GI neurons were not changed in the shRNA-treated group. Our data suggest that hypothalamic prostaglandins are critical for recovering from acute hypoglycemia by affecting glucose-sensing neurons. Hypothalamic prostaglandins are also essential to develop an attenuation of CRRs during RH.

Main

Medications for diabetes often lead to hypoglycemia as a side effect, leading to lightheadedness, fainting, and even death. Hypoglycemia-related death is increasing worldwide[1]. The development of continuous glucose monitoring systems revealed that hypoglycemia occurs more often than expected[2]. Hypoglycemia increases glucagon, corticosteroids, and catecholamine secretions to enhance hepatic glucose production and restore glucose levels[3]. These responses are called counter-regulatory responses (CRRs). The hypothalamus is a vital brain region in regulating glucose metabolism[4]. Various cores of the hypothalamus, such as the paraventricular nucleus of the hypothalamus, the ventromedial nucleus of the hypothalamus (VMH), and the arcuate nucleus of the hypothalamus (ARC), have been reported to regulate systemic glucose metabolism, regulating insulin secretion from the pancreas, changing insulin sensitivity in muscle and liver, and releasing CRR hormones[3–5]. Among them, the VMH is known to regulate CRRs[5]. Electrical or chemogenetic activation of the VMH increases blood glucose levels[6,7]. Neuronal circuits from the lateral parabrachial nucleus (PBN) to the VMH and VMH to the bed nucleus of the stria terminalis (BNST) regulate CRRs during hypoglycemia[8–10].

There are two types of glucose-sensing neurons in the brain: glucose-inhibited (GI) neurons and glucose-excited (GE) neurons. GI neurons are activated by hypoglycemia and increase glucose production from the liver by changing CRRs[5]. A subset of neuropeptide Y neurons in the ARC[11], hypocretin/orexin neurons in the lateral hypothalamus[12], cholecystokinin (CCK)- or leptin receptor-expressing neurons in the PBN of the pons[9,10] have GI characteristic. In the VMH, pituitary adenylate-cyclase-activating polypeptide[13], glucokinase[14], nitric oxide synthase 1 (NOS1)[8], CCK B receptor[15], anoctamin 4 channel-positive neurons[16] are GI and have the potential to increase blood

glucose. It is known that low glucose levels increase AMP-activated protein kinase activity and nitrogen oxide to activate GI neurons in the hypothalamus[17]. Lactate infusion into the VMH during hypoglycemia attenuates CRRs[18]. In contrast, GE neurons regulate insulin sensitivity in peripheral tissues during hyperglycemia[19,20]. K_{ATP} channel in the GE neuron affects CRRs during hypoglycemia[21]. Recently, we have reported that high blood glucose increases prostaglandin production in the hypothalamus and activates GE neurons[19]. Prostaglandins modulate ion channel activity and thus change insulin secretion[22,23]. Non-steroidal anti-inflammatory drugs (NSAIDs) inhibit the K_{ATP} channel and increase insulin secretion[24]. NSAIDs also affect hepatocytes to decrease gluconeogenesis[25]. Thus, NSAIDs induce hypoglycemia when used together with anti-diabetic drugs[26]. Insulin-induced hypoglycemia inhibits the incorporation of arachidonic acid into phospholipids in the brain[27]. Hypoxia-hypoglycemia activates phospholipase A2 (PLA2), increases the release of arachidonic acid, and increases cFos in neuroblastoma cells[28]. However, the role of hypothalamic prostaglandin in CRRs during hypoglycemia is unclear.

Recurrent hypoglycemia (RH), characterized by experiencing hypoglycemia multiple times, attenuates CRRs. RH increases the risk of dementia[29]. Central and peripheral mechanisms of the attenuation have been reported[30]. In the central nervous system, RH affects GE and GI neurons' sensitivity to glucose[31]. Lactate production from glycogen in astrocytes in the VMH also affects the development of RH[18]. Lactate is utilized as an alternative fuel in the brain after RH[32]. However, the role of hypothalamic prostaglandin in RH has also not been reported.

In this study, our aim was to investigate the impact of hypoglycemia on prostaglandin production in the hypothalamus and the effects of prostaglandin on CRRs under both acute hypoglycemia and RH. Our data indicate that hypoglycemia can change phospholipid metabolism to produce prostaglandins in the hypothalamus, which is necessary to enhance neuronal activity in the ventrolateral part of the VMH and glucagon secretion during hypoglycemia. Inhibition of phospholipid metabolism by short-hairpin RNA (shRNA) against cytosolic PLA2 (cPLA2) in the hypothalamus improves the attenuation of CRRs during RH.

Results

Glucose deprivation, induced by insulin and 2DG, decreases arachidonic acid-containing phospholipids in the hypothalamus in mice

To check the role of hypoglycemia in hypothalamic phospholipid metabolism, mice received insulin injection intraperitoneally (i.p.) and the signal intensity of 11 different phospholipids located in both the VMH and the ARC were measured at 30 min after the insulin injection (Fig. 1a, b and Table S1). Insulin injection decreased phosphatidylinositol (PI) (16:0/20:4), PI (18:0/20:4), PI (18:1/20:4), phosphatidylethanolamine (PE) (18:0/16:1), PE (18:0/20:4) and phosphatidylserine (PS) (18:0/16:0) compared to the saline group in the VMH (Fig. 1b-e) and PI (16:0/20:4), PI (18:0/20:4), and PI (18:1/20:4) in the ARC (Fig. 1b, f-h). Phospholipids are metabolized by PLA1, PLA2, PLC, and PLD. Insulin injection activated cPLA2 but not secretory PLA2 in the hypothalamus (Fig. 1i-j).

To further study the role of insulin in hypothalamic phospholipid metabolism, we used streptozotocin (STZ) to disrupt the pancreatic beta cells and insulin secretion. When phospholipid intensity was examined in the VMH and ARC of the mice 4 days after receiving STZ injection, no significant differences were observed in any types of phospholipids, including PI, PE, and PS in either hypothalamic nucleus (Fig. 2a-f and Table S1). 2-Deoxy-d-glucose (2DG) cannot be metabolized in glycolysis and causes glucose deprivation in the cell. I.p. injection of 2DG decreased the signal intensity of PI (18:0/20:4) and PE (p18:0/20:4) in the VMH compared to mice receiving a saline injection (Fig. 2g-i). 2DG injection also decreased PI (18:1/20:4), PE (p18:0/20:4) and PS (18:0/16:0) in the ARC (Fig. 2j-l). These data suggest that not only insulin but also hypoglycemia enhances arachidonic acid (AA)-containing phospholipid metabolism in the hypothalamus, at least in part.

Insulin increases prostaglandin production in the hypothalamus

AA is known to be used as a substrate of prostaglandins (PGs). Thus, we measured all types of PGs in the whole hypothalamus 30 min after insulin injection by liquid chromatography/mass spectrometry (LC-MS). Insulin injection increased the amount of 6-keto-PGF1α, 11-β-13,14-dihydro-15-keto-PGF2α, PGF2α, PGE2, and 20-hydroxy-PGF2α in the hypothalamus (Fig. 3a-f). Therefore, these results suggest that insulin injection induces AA release from phospholipids to produce PGs in the hypothalamus.

Ibuprofen blocks CRRs and activity of GI neuron

To investigate the role of PGs in the brain in regulating systemic glucose metabolism, we injected ibuprofen intracerebroventricularly (i.c.v.) and measured glucose production induced by i.p. injection of 2DG. 2DG injection activates CRRs and increased blood glucose levels (Fig. 4a, b). I.c.v. injection of ibuprofen lowered the 2DG-induced hyperglycemia (Fig. 4a, b). 2DG is also known to increase food intake. However, ibuprofen injection did not change feeding behavior compared to saline-injected mice (Fig. 4c).

To verify the role of PGs in the CRRs, we performed hyperinsulinemic-hypoglycemic clamp experiments in mice. In the hypoglycemic clamp, a constant rate of insulin (10 mU/kg/min) was infused into the circulation, while glucose was infused as needed to maintain blood glucose levels at 50 mg/dL (Fig. 4d). Ibuprofen injection into the VMH increased glucose infusion rate (GIR) (Fig. 4e), suggesting that ibuprofen inhibited glucose production during hypoglycemia and thus, more glucose was needed to maintain at 50 mg/dL. Then, we measured CRRs-related hormones in the blood at 120 min of the clamp experiment. Ibuprofen injection significantly decreased glucagon levels but not corticosterone, epinephrine, and norepinephrine (NE) (Fig. 4f-i). These data suggest that hypothalamic PGs are necessary for glucagon secretion in response to hypoglycemia to induce glucose production. Hypothalamic GI neurons regulate CRRs. Insulin (i.p.) significantly increased the number of cFos-positive cells in the ventrolateral part of the VMH (vlVMH), while oral injection of ibuprofen suppressed it (Fig. 5a, b). The number of cFos-positive cells was not altered by ibuprofen injection in the dorsomedial (dm) and central (c) part of the VMH and ARC (Fig. 5a-c).

RH attenuates glucose production, but preserves hypothalamic glucose metabolism during hypoglycemia

To generate the RH mouse model, 2.5 U/kg of insulin was injected i.p. once a day for 5 days to induce hypoglycemia (40 mg/dL) (Fig. 6a). On day 6, hypoglycemic clamp was performed (Fig. 6b). GIR was significantly increased in RH mice (Fig. 6c), suggesting that RH attenuated CRR-related glucose production. In the control mice, insulin-induced hypoglycemia decreased intermediates of

glycolysis and lactate content in the hypothalamus (Fig. 6d). Intermediates of tricarboxylic acid (TCA) cycle were not changed by insulin injection (Fig. 6e). Amino acids, such as alanine, serine, threonine, phenylalanine, arginine, proline, and methionine, in the hypothalamus were lower after insulin injection (Fig. 6f). NE content, but not glutamate and γ-aminobutyric acid (GABA), in the hypothalamus was deceased after insulin injection (Fig. 6g). However, changes in all of the metabolites, except for glucose, were not observed in RH mice after insulin injection (Fig. 6h-j), suggesting that some adaptation occurred to prevent energy deprivation in the hypothalamus after RH. NE was also not changed by insulin after RH (Fig. 6k).

Hypothalamic cPLA2 attenuates glucose production during RH

To inhibit the production of PGs in the hypothalamus, which may be derived from AA in phospholipids, we injected shRNA against cPLA2 (shPLA2) into the VMH (Fig. 7a). Adeno-associated virus (AAV)-infected cells were found in the vlVMH and ARC (Fig. 7b). cPLA2 mRNA in the hypothalamus was significantly decreased (Fig. 7c). shPLA2 mice received RH treatment for 5 days and hypoglycemic clamp was performed (Fig. 7d-f). GIR in the shPLA2 without RH was similar to that of control-RH mice and ibuprofen-injected mice (Fig. 4e, 6c, 7g), confirming that hypothalamic PG production enhances CRRs. However, the shPLA2 inhibited the increase in GIR after RH (Fig. 7g). RH decreased plasma glucagon and epinephrine at 120 min in the hypoglycemic clamp (Fig. 7h, i). shPLA2 did not improve glucagon, epinephrine, NE, and corticosterone levels (Fig. 7h-k). RH did not change the numbers of Iba1, GFAP, and cFos positive cells in the VMH (Fig. 7l-o).

Discussion

This study shows that insulin, possibly insulin-induced hypoglycemia, increases PG production using arachidonic acid from phospholipids, at least partially. The PG production in the VMH was necessary for the hypoglycemia-induced neuronal activation in the vlVMH, glucagon secretion from the pancreas, and an increase in hepatic glucose production. RH attenuates CRRs but improves hypothalamic energy deprivation during hypoglycemia. Phospholipid metabolism by cPLA2 is critical for attenuating glucose production in RH, but the mechanism is unclear.

NSAIDs, including salicylates, were used to treat diabetic patients in the early 1900s[33]. NSAIDs cause gastrointestinal bleeding[33] and severe hypoglycemia when used with other blood glucose-lowering agents[26]. Hence, they are no longer used as anti-diabetic drugs. The mechanism of the hypoglycemic effect of NSAIDs has been studied only in the peripheral tissues[24,25]. While NSAIDs are the most commonly used drug for analgesics due to their inhibition of PG production in the brain, research on their effect on lowering blood glucose levels in the central nervous system is limited. I.c.v. injection of PGD2, PGE1, PGE2, or PGF2α increases the glucose concentration in the hepatic vein[34]. PGF2α has the most substantial effect but is mediated by epinephrine secretion from the adrenal medulla, not glucagon[34].

The VMH plays a vital role in the regulation of CRRs to hypoglycemia. A lesion of the VMH suppresses CRRs in response to systemic injection of 2DG[35]. 2DG perfusion in the VMH via microdialysis increases glucagon, epinephrine, and NE secretion[36]. In contrast, glucose perfusion in the VMH during the hypoglycemic clamp blocks increases the secretion of CRR-related hormones[37]. Synaptic glutamate release from the VMH-specific steroidogenic factor 1 (SF1) neuron regulates CRRs[38]. Neuronal pathways from the PBN to the VMH[9] and from VMH to the BNST regulate CRRs[39]. Therefore, it is considered that the VMH has a sensor to detect low blood glucose levels and change CRRs. Both GI and GE neurons of estrogen receptor alpha (ERα)-expressing neurons are involved in the CRRs[40]. In the present data, we found that ibuprofen affects neuronal activity in the vlVMH but not dmVMH and cVMH. The specific neurons responsible for NSAID-related hypoglycemia remain to be studied. In our previous paper[19], the knockdown of cPLA2 in SF1 neurons did not change blood glucose levels after systemic 2DG injection compared to control mice. Therefore, neurons in the dmVMH, including SF1 neurons, may not be necessary for NSAID-related change in CRRs. In ERα-expressing neurons that localize mainly in the vlVMH, both GI-type ERα

neurons projecting to the medioposterior ARC and GE-type ERα neurons projecting to the dorsal raphe nucleus regulate CRRs[41]. Thus, similar neuronal circuits may regulate NSAID-related hypoglycemia, but our study did not identify the downstream neurons of vlVMH.

Recently, the importance of glucagon in both type 1 and type 2 diabetes mellitus (T1DM, T2DM) is apparent[42]. In our study, intra-hypothalamic injection of ibuprofen decreased glucagon secretion during hypoglycemia. In T2DM patients, NSAIDs decreased blood glucose concentration and HbA1c[43,44]. In a retrospective cohort study, NSAIDs also reduced the risk of becoming T2DM[45]. Since glucagon concentrations were not measured in these papers, the relationship between NSAIDs, glucagon, and T2DM is still unclear. Further study is needed to clarify the mechanisms by which NSAIDs improve T1 and T2DM.

In our metabolomic data, insulin lowered glycolytic intermediates and lactate but not intermediates of the TCA cycle in control mice. Insulin also decreased amino acids, so they may be utilized in the TCA cycle. Glucagon regulates amino acid catabolism in the liver to enhance gluconeogenesis[45]. Glucagon may enhance it in the hypothalamus as well. GABA and NE release in the VMH is increased by hypoglycemia and regulates CRRs[18,46]. In our data, insulin decreased NE content but not GABA content. The decrease may be due to the higher release of NE.

RH is a critical incident in the treatment of diabetes, and it can result in hypoglycemia-associated autonomic failure. RH increases hexokinase activity and attenuates the activity of glucose-sensing neurons in the VMH[47,48]. RH also increases lactate production and utilization in the brain[32], but it is speculated that using only lactate instead of glucose may not be sufficient for the whole energy demand of the brain[49]. In our metabolomic data, RH did not decrease PEP, lactate, pyruvic acid, amino acids, and even NE, suggesting that some metabolic adaptations occurred to maintain intracellular energy metabolism. The levels of glucagon and epinephrine were lower in our RH mice, possibly indicating that the hypothalamic energy status was not hypoglycemic, as suggested by our metabolomic data. Consequently, it is conceivable that GI neurons may not be functioning to recover hypoglycemia. cFos in the VMH was not deceased in the control-RH group, suggesting that other brain regions may be important for RH-CRRs. GE neurons may affect RH-CRRs, but it is challenging to observe the decreased activity in GE by cFos. One of the lactate-producing sites is astrocytes, and astrocytic glycogen is important for lactate production during RH[50]. RH increases fatty acid oxidation in human astrocytoma cells[51]. Hypothalamic microglia is

activated by hypoglycemia and impairs epinephrine release[52]. However, the numbers of GFAP and Iba1 positive cells in the VMH were not changed in our RH model. When shPLA2 mice underwent the RH procedure, shPLA2 in the vlVMH inhibits the attenuation of CRRs. However, the RH-induced decline in glucagon and epinephrine levels during hypoglycemic clamp were not improved. Hypothalamic shPLA2 may suppress another mechanism induced by RH, such as increasing adrenergic sensitivity in the liver and visceral fat[53].

The present study revealed the importance of PGs in the hypothalamus for the recovery from hypoglycemia. Hypothalamic PGs regulate the activity of GI neurons and enhance glucagon secretion. RH, which induces metabolic adaptation in the hypothalamus, impairs glucagon and epinephrine secretion. Hypothalamic PGs attenuate glucose production after RH with unidentified mechanisms. More studies are needed to broaden our understanding of strategies to prevent RH.

References

1. Zaccardi, F., Dhalwani, N. N., Webb, D. R., Davies, M. J. & Khunti, K. Global burden of hypoglycaemia-related mortality in 109 countries, from 2000 to 2014: an analysis of death certificates. *Diabetologia* **61**, 1592–1602 (2018).
2. Gehlaut, R. R., Dogbey, G. Y., Schwartz, F. L., Marling, C. R. & Shubrook, J. H. Hypoglycemia in Type 2 Diabetes - More Common Than You Think. *J. Diabetes Sci. Technol.* **9**, 999–1005 (2015).
3. Verberne, A. J. M., Sabetghadam, A. & Korim, W. S. Neural pathways that control the glucose counterregulatory response. *Frontiers in Neuroscience* vol. 8 (2014).
4. Pozo, M. & Claret, M. Hypothalamic Control of Systemic Glucose Homeostasis: The Pancreas Connection. *Trends Endocrinol. Metab.* **29**, 581–594 (2018).
5. Shimazu, T. & Minokoshi, Y. Systemic Glucoregulation by Glucose-Sensing Neurons in the Ventromedial Hypothalamic Nucleus (VMH). *J. Endocr. Soc.* **1**, 449–459 (2017).
6. Sudo, M., Minokoshi, Y. & Shimazu, T. Ventromedial hypothalamic stimulation enhances peripheral glucose uptake in anesthetized rats. *Am. J. Physiol. Metab.* **261**, E298–E303 (1991).
7. Coutinho, E. A. *et al.* Activation of SF1 Neurons in the Ventromedial Hypothalamus by DREADD Technology Increases Insulin Sensitivity in Peripheral Tissues. *Diabetes* **66**, 2372–

2386 (2017).

8. Faber, C. L. *et al.* Distinct Neuronal Projections From the Hypothalamic Ventromedial Nucleus Mediate Glycemic and Behavioral Effects. *Diabetes* **67**, 2518–2529 (2018).

9. Flak, J. N. *et al.* Leptin-inhibited PBN neurons enhance responses to hypoglycemia in negative energy balance. *Nat. Neurosci.* **17**, 1744–1750 (2014).

10. Garfield, A. S. *et al.* A Parabrachial-Hypothalamic Cholecystokinin Neurocircuit Controls Counterregulatory Responses to Hypoglycemia. *Cell Metab.* **20**, 1030–1037 (2014).

11. Muroya, S., Yada, T., Shioda, S. & Takigawa, M. Glucose-sensitive neurons in the rat arcuate nucleus contain neuropeptide Y. *Neurosci. Lett.* **264**, 113–116 (1999).

12. Yamanaka, A. *et al.* Hypothalamic Orexin Neurons Regulate Arousal According to Energy Balance in Mice. *Neuron* **38**, 701–713 (2003).

13. Khodai, T. *et al.* PACAP Neurons in the Ventromedial Hypothalamic Nucleus Are Glucose Inhibited and Their Selective Activation Induces Hyperglycaemia. *Front. Endocrinol. (Lausanne).* **9**, (2018).

14. Stanley, S. A. *et al.* Bidirectional electromagnetic control of the hypothalamus regulates feeding and metabolism. *Nature* **531**, 647–650 (2016).

15. Flak, J. N. *et al.* Ventromedial hypothalamic nucleus neuronal subset regulates blood glucose independently of insulin. *J. Clin. Invest.* **130**, 2943–2952 (2020).

16. Tu, L. *et al.* Anoctamin 4 channel currents activate glucose-inhibited neurons in the mouse ventromedial hypothalamus during hypoglycemia. *J. Clin. Invest.* **133**, (2023).

17. Murphy, B. A., Fakira, K. A., Song, Z., Beuve, A. & Routh, V. H. AMP-activated protein kinase and nitric oxide regulate the glucose sensitivity of ventromedial hypothalamic glucose-inhibited neurons. *Am. J. Physiol. Physiol.* **297**, C750–C758 (2009).

18. Chan, O., Paranjape, S. A., Horblitt, A., Zhu, W. & Sherwin, R. S. Lactate-Induced Release of GABA in the Ventromedial Hypothalamus Contributes to Counterregulatory Failure in Recurrent Hypoglycemia and Diabetes. *Diabetes* **62**, 4239–4246 (2013).

19. Lee, M. L. *et al.* Prostaglandin in the ventromedial hypothalamus regulates peripheral glucose metabolism. *Nat. Commun.* **12**, 1–15 (2021).

20. Toda, C. *et al.* UCP2 Regulates Mitochondrial Fission and Ventromedial Nucleus Control of Glucose Responsiveness. *Cell* **164**, 872–883 (2016).

21. Evans, M. L. *et al.* Hypothalamic ATP-sensitive K + Channels Play a Key Role in Sensing Hypoglycemia and Triggering Counterregulatory Epinephrine and Glucagon Responses. *Diabetes* **53**, 2542–2551 (2004).

22. Meves, H. The action of prostaglandins on ion channels. *Curr. Neuropharmacol.* **4**, 41–57 (2006).

23. Carboneau, B. A., Breyer, R. M. & Gannon, M. Regulation of pancreatic β-cell function and mass dynamics by prostaglandin signaling. *J. Cell Commun. Signal.* **11**, 105–116 (2017).

24. Li, J. *et al.* Non-steroidal anti-inflammatory drugs increase insulin release from beta cells by inhibiting ATP-sensitive potassium channels. *Br. J. Pharmacol.* **151**, 483–493 (2007).

25. Yan, S. *et al.* I Prostanoid Receptor–Mediated Inflammatory Pathway Promotes Hepatic Gluconeogenesis Through Activation of PKA and Inhibition of AKT. *Diabetes* **63**, 2911–2923 (2014).

26. Sone, H., Takahashi, A. & Yamada, N. Ibuprofen-Related Hypoglycemia in a Patient Receiving Sulfonylurea. *Ann. Intern. Med.* **134**, 344 (2001).

27. Strosznajder, J. Effect of hypoglycemia on the brain free fatty acid level and the uptake of fatty acids by phospholipids. *Neurochem. Res.* **9**, 465–476 (1984).

28. Petroni, A., Papini, N., Blasevich, M., Rise, P. & Galli, C. Arachidonate release and c-fos expression in various models of hypoxia and hypoxia–hypoglycemia in retinoic acid differentiated neuroblastoma cells. *Neurochem. Int.* **40**, 255–260 (2002).

29. Mehta, H. B., Mehta, V. & Goodwin, J. S. Association of Hypoglycemia With Subsequent Dementia in Older Patients With Type 2 Diabetes Mellitus. *Journals Gerontol. Ser. A Biol. Sci. Med. Sci.* glw217 (2016) doi:10.1093/gerona/glw217.

30. LaGamma, E. F., Kirtok, N., Chan, O. & Nankova, B. B. Partial blockade of nicotinic acetylcholine receptors improves the counterregulatory response to hypoglycemia in recurrently hypoglycemic rats. *Am. J. Physiol. Metab.* **307**, E580–E588 (2014).

31. Fioramonti, X., Song, Z., Vazirani, R. P., Beuve, A. & Routh, V. H. Hypothalamic Nitric Oxide in Hypoglycemia Detection and Counterregulation: A Two-Edged Sword. *Antioxid. Redox Signal.* **14**, 505–517 (2011).

32. Herzog, R. I. *et al.* Lactate preserves neuronal metabolism and function following antecedent recurrent hypoglycemia. *J. Clin. Invest.* **123**, 1988–1998 (2013).

33. Vue, M. H. & Setter, S. M. Drug-Induced Glucose Alterations Part 1: Drug-Induced Hypoglycemia. *Diabetes Spectr.* **24**, 171–177 (2011).

34. YATOMI, A. *et al.* Prostaglandins Affect the Central Nervous System to Produce Hyperglycemia in Rats*. *Endocrinology* **121**, 36–41 (1987).

35. Borg, W. P. *et al.* Ventromedial hypothalamic lesions in rats suppress counterregulatory responses to hypoglycemia. *J. Clin. Invest.* **93**, 1677–1682 (1994).

36. Borg, W. P., Sherwin, R. S., During, M. J., Borg, M. A. & Shulman, G. I. Local Ventromedial Hypothalamus Glucopenia Triggers Counterregulatory Hormone Release. *Diabetes* **44**, 180–184 (1995).

37. Borg, M. A., Sherwin, R. S., Borg, W. P., Tamborlane, W. V & Shulman, G. I. Local ventromedial hypothalamus glucose perfusion blocks counterregulation during systemic hypoglycemia in awake rats. *J. Clin. Invest.* **99**, 361–365 (1997).

38. Tong, Q. *et al.* Synaptic Glutamate Release by Ventromedial Hypothalamic Neurons Is Part of the Neurocircuitry that Prevents Hypoglycemia. *Cell Metab.* **5**, 383–393 (2007).

39. Meek, T. H. *et al.* Functional identification of a neurocircuit regulating blood glucose. *Proc. Natl. Acad. Sci.* **113**, (2016).

40. Saito, K. *et al.* Visualizing estrogen receptor-α-expressing neurons using a new ERα-ZsGreen reporter mouse line. *Metabolism* **65**, 522–532 (2016).

41. He, Y. *et al.* Estrogen receptor-α expressing neurons in the ventrolateral VMH regulate glucose balance. *Nat. Commun.* **11**, 2165 (2020).

42. Lee, Y. H., Wang, M.-Y., Yu, X.-X. & Unger, R. H. Glucagon is the key factor in the development of diabetes. *Diabetologia* **59**, 1372–1375 (2016).

43. Goldfine, A. B. Salicylate (Salsalate) in Patients With Type 2 Diabetes. *Ann. Intern. Med.* **159**, 1 (2013).

44. Faghihimani, E. *et al.* Salsalate improves glycemic control in patients with newly diagnosed type 2 diabetes. *Acta Diabetol.* **50**, 537–543 (2013).

45. Lin, M.-H. *et al.* Association between Non-Steroidal Anti-Inflammatory Drugs Use and the Risk of Type 2 Diabetes Mellitus: A Nationwide Retrospective Cohort Study. *J. Clin. Med.* **11**, 3186 (2022).

46. Barnes, M. B., Lawson, M. A. & Beverly, J. L. Rate of fall in blood glucose and recurrent

hypoglycemia affect glucose dynamics and noradrenergic activation in the ventromedial hypothalamus. *Am. J. Physiol. Integr. Comp. Physiol.* **301**, R1815–R1820 (2011).

47. Osundiji, M. A. *et al.* Recurrent hypoglycemia increases hypothalamic glucose phosphorylation activity in rats. *Metabolism* **60**, 550–556 (2011).

48. Kang, L. *et al.* Prior hypoglycemia enhances glucose responsiveness in some ventromedial hypothalamic glucosensing neurons. *Am. J. Physiol. Integr. Comp. Physiol.* **294**, R784–R792 (2008).

49. McCrimmon, R. J. Consequences of recurrent hypoglycaemia on brain function in diabetes. *Diabetologia* **64**, 971–977 (2021).

50. Su, G. *et al.* Astrocyte Glycogen Is a Major Source of Hypothalamic Lactate in Rats With Recurrent Hypoglycemia. *Diabetes* **72**, 1154–1160 (2023).

51. Weightman Potter, P. G. *et al.* Basal fatty acid oxidation increases after recurrent low glucose in human primary astrocytes. *Diabetologia* **62**, 187–198 (2019).

52. Winkler, Z. *et al.* Hypoglycemia-activated Hypothalamic Microglia Impairs Glucose Counterregulatory Responses. *Sci. Rep.* **9**, 6224 (2019).

53. Liu, Z. *et al.* Recurrent hypoglycemia increases hepatic gluconeogenesis without affecting glycogen metabolism or systemic lipolysis in rat. *Metabolism* **136**, 155310 (2022).

54. Yamada, M. *et al.* A comprehensive quantification method for eicosanoids and related compounds by using liquid chromatography/mass spectrometry with high speed continuous ionization polarity switching. *J. Chromatogr. B* **995**–**996**, 74–84 (2015).

55. Arima, Y. *et al.* Murine neonatal ketogenesis preserves mitochondrial energetics by preventing protein hyperacetylation. *Nat. Metab.* **3**, 196–210 (2021).

METHODS

Animals

C57L/6N male and female mice (The Jackson Laboratory Japan, Yokohama, Japan) were kept at room temperature with a 12h/12h day light and dark time cycle. The mice had free access to water and regular chow diet (Nosan Corporation, Yokohama, Japan). Experiments were carried out in the Experimental Animal Facility of Hokkaido University (AAALAC Accredited) and Kumamoto

University. Mice cages were changed once a week, and mice care was performed according to the Animal Care and Use Committee guidelines of Hokkaido University and Kumamoto University.

Recurrent hypoglycemia

C57L/6N male and female mice received i.p. injection of insulin (2.5 U/kg, Humarin R, Eli Lilly Japan, Hyogo, Japan) at 1 pm. Blood glucose levels were measured by a handy glucose meter (Nipro FreeStyle, Nipro, Osaka, Japan). When blood glucose level reached 40 mg/dL, glucose (3 g/kg) was injected i.p. or subcutaneously to rescue from hypoglycemia. The same procedure was repeated 5 times.

Imaging mass spectrometry

C57BL male mice received i.p. injection of insulin, 2DG (2 g/kg body weight, Sigma-Aldrich, St. Louis, MO), or saline, after which they were sacrificed using CO_2 asphyxiation 30 min after injection. The mice brains were immediately placed into ice-cold saline, embedded in 2% sodium carboxymethyl cellulose solution, and frozen with liquid nitrogen. The 10-μm brain sections were prepared by cryostat and immediately mounted onto an indium-tin-oxide-coated glass slide (Bruker Daltonics, Bremen, Germany). The sections on the glass slides were immediately dried and stored at −20°C until imaging mass spectrometry analysis.

The brain sections were sprayed with 9-aminoacridine matrix (10 mg/mL in 70% ethanol, Sigma-Aldrich) and installed into a matrix-assisted laser desorption/ionization (MALDI)-time-of-flight (TOF)/TOF system using ultrafleXtreme (Bruker Daltonics). The brain sections were irradiated by a smart beam (Nd: YAG laser, 355-nm wavelength), with a 25-μm irradiation pitch. The laser had a repetition frequency of 2000 Hz and mass spectra were obtained in the range of m/z 200–1200 in negative-ion mode. The m/z values from previous reports were used to label each lipid, phospholipid, and lyso species. All ion images were reconstructed with total ion current (TIC) normalization by flexImaging (Bruker Daltonics) and transferred to ImageJ software after modifying the grayscale. The areas of the VMH were identified by 4’,6-diamidino-2-phenylindole (DAPI) staining in the other brain sections, and the brightness of mass spectrometry signals in the VMH and ARC were calculated as intensity. Phosphatidyl-choline and phosphatidyl-glycerol were measured in the adjacent tissue sections with positive-ion mode. However, the mass spectra after

MS/MS were inconclusive enough to allow a reliable data assignment, especially for fatty acid components.

Quantification of PGs

C57BL male mice received i.p. injection of insulin, 2DG (2 g/kg body weight, Sigma-Aldrich), or saline, after which they were sacrificed using CO_2 asphyxiation at t = 30 min. The hypothalamus was collected and immediately frozen in liquid nitrogen. The tissue was homogenized with 500 μL of methanol: formic acid (100:0.2) containing an internal standard consisting of a mixture of deuterium-labeled PGs using microtip sonication. The samples were subjected to solid phase extraction using an Oasis HLB cartridge (5 mg; Waters, Milford, MA)[54]. Samples were diluted with water: formic acid (100:0.03) to give a final methanol concentration of ~20% by volume, applied to preconditioned cartridges, and serially washed with water: formic acid (100:0.03), water: ethanol: formic acid (90:10:0.03), and petroleum ether. Samples were eluted with 200 μL of methanol: formic acid (100:0.2). The filtrate was concentrated with a vacuum concentrator (SpeedVac, Thermo Fisher Scientific, Waltham, MA). The concentrated filtrate was dissolved in 50 μL of methanol and used for liquid chromatography/mass spectrometry (LC-MS).

The PGs in the hypothalamus were quantified by liquid chromatography/mass spectrometry[54]. A triple-quadrupole mass spectrometer equipped with an electrospray ionization (ESI) ion source (LCMS-8040, Shimadzu Corporation, Kyoto, Japan) was used in the positive and negative-ESI and selective reaction monitoring modes. The samples were resolved on a reversed-phase column (Kinetex C8, 2.1 × 150 mm, 2.6 μm, Phenomenex, Torrance, CA) using a step gradient with mobile phase A (0.1% formic acid) and mobile phase B (acetonitrile). The gradient of mobile phase B concentration was programmed as 10% (0 min)−25% (5 min)−35% (10 min)−75% (20 min)−95% (20.1 min)−95% (28 min)−10% (28.1 min)−10% (30 min), at a flow rate of 0.4 mL/min and a column temperature of 40°C.

Focused microwave (FMW) and GC-MS for metabolome measurement

C57BL female mice received i.p. injection of insulin (1 U/kg) or saline. After 30 min, the mice were sacrificed in FMW under deep anesthesia with 3% isoflurane (FUJIFILM Wako Pure Chemical Corporation, Osaka, Japan). The mice were placed in the MUROMACHI MICROWAVE FIXATION

SYSTEM (MODEL MMW-05, Muromachi Kikai, Tokyo Japan). The mice brains were microwave-irradiated at 2.00 kw for 1.10 s. The brains were collected, and -1.0 to -2.0 mm coronal sections from the bregma were excised using the matrix, and the VMH and ARC areas were sampled under the microscope.

The hypothalamic samples were used for metabolome measurement as reported previously[55]. The samples were plunged into Milli-Q water/methanol/chloroform (at a ratio of 1:2.5:1) containing internal standards (isopropylmalic acid). The samples were homogenized at 2,300 r.p.m. for 30 s with a bead beater-type homogenizer (Beads crusher μT-12, Titec, Saitama, Japan). The homogenized samples were shaken at 1,200 r.p.m. and 37°C for 30 min and centrifuged at 16,000 × *g* and 4°C for 3 min. Subsequently, 225 μL of the upper aqueous layer was transferred to a new tube. The remaining samples were mixed with 200 μL Milli-Q water and centrifuged again at 16,000 × *g* and 4°C for 3 min. The solution was evaporated using a centrifugal evaporator (DNA120OP230, Thermo Fisher Scientific) and lyophilized (FD-1-84A, FST). The samples were derivatized with methoxamine/ pyridine and N-methyl-N-trimethylsilyl-trifluoroacetamide and analyzed on a TQ8050 GC–MS/MS (Shimadzu Corporation). The chromatograms and mass spectra were analyzed utilizing the GC–MS solution software v4.50 (Shimadzu Corporation). Compounds were determined with the Smart Metabolites Database v2 (Shimadzu Corporation).

Cannula implantation and AAV injection

C57BL male mice were anesthetized with ketamine (100 mg/kg) and xylazine (10 mg/kg) or a combination anesthetic (0.3 mg/kg of medetomidine, 4.0 mg/kg of midazolam, and 5.0 mg/kg of butorphanol). The mice were placed on the stereotaxic instrument (Narishige, Tokyo, Japan). The mice skulls were opened with a Cranial drill (dental drill). A stainless steel cannula (Plastics One, P1 Technologies, VA, USA) was inserted into the VMH using the following coordinates: an anterior-posterior (AP) direction; −1.5 (1.5 mm posterior to the bregma), lateral (L): ±0.4 (0.4 mm lateral to the bregma), dorsal-ventral (DV): −5.7 (5.7 mm below the bregma on the surface of the skull). The interval between the two cannulae was 0.8 mm, so there would be 0.4 mm on both sides. For i.c.v., AP: − 0.3, L: 1.0, DV: −2.0. Cannulae were secured on the skulls with cyanoacrylic glue and the exposed skulls were covered with dental cement. For AAV injection, the mice were injected in each side of the VMH with a maximum of 0.3 μL AAV9-RFP-U6-m-PLA2G4A-shRNA (1.0×10^{12} GC/mL,

shAAV-268768, Vector Biolabs, PA, USA) bilaterally using the following coordinates: AP: − 1.5, L: ± 0.5, DV: − 5.7. Open wounds were sutured after the viral injection. The mice were allowed to recover for 5–7 days before experiments were started.

Quantitative real-time-PCR was performed to assess the efficiency of shPLA2 in the hypothalamus. Mice were anesthetized with isoflurane, and their brains were collected immediately, after which the hypothalamus was trimmed using a brain matrix. The hypothalamus was homogenized with Template Prepper (Nippon Gene, Tokyo, Japan), and the extracted RNA was reverse-transcribed using Oligo(dT)18 primer (Thermo Fisher Scientific) and M-MLV Reverse Transcriptase (Promega, Madison, WI). *Pla2g4a* and *Actin B* cDNA levels in the hypothalamus were measured by ΔΔCt method using SYBR Green reagent (Bio-Rad, Hercules, CA). The information on primers is shown in table S1. Quantitative PCR was performed with diluted cDNAs in a 10 µl reaction volume in duplicate.

Assessment of cytosolic- or secretory-phospholipase-A2 activity

C57BL male mice fed *ad libitum* were i.p. injected with either insulin (1 U/kg) or saline. The mice were sacrificed 30 min after the injection using CO_2 asphyxiation and a -1.0 to -2.0 mm coronal section from the bregma was excised using the matrix, and the VMH and ARC areas were collected and stored at −80°C until use. Tissues were homogenized and centrifuged at 10,000 × *g* for 15 min at 4°C and supernatants were collected. The activity of cytosolic- or secretory-phospholipase-A2 was measured according to the procedures described in the kit manuals (Abcam, Cambridge, UK).

2DG-induced hyperglycemia and food intake

Ibuprofen (50 µg in 0.5 µL) or vehicle [20% dimethyl sulfoxide (DMSO) in phosphate-buffered saline (PBS)] was injected through the i.c.v cannulae in C57BL/6N mice in fed state 30 min before the i.p. injection of 2-DG (300 mg/kg). Blood glucose levels were measured by the handheld glucometer (Nipro FreeStyle, Nipro, Osaka, Japan) at -30, 0, 15, 30, 60, 90, and 120 min. For food intake, i.c.v. injection of ibuprofen and i.p. injection of 2-DG were performed as described above. The reduced weight of food was measured at time points of 0, 15, 30, 60, 90, 120, 150, and 180 min.

Hyperinsulinemic-hypoglycemic clamp

C57BL male mice were anesthetized with pre-mixed ketamine (100 mg/kg) and xylazine (10 mg/kg) or a combination anesthetic (0.3 mg/kg of medetomidine, 4.0 mg/kg of midazolam, and 5.0 mg/kg of butorphanol). Polyethylene catheters were implanted into right carotid arteries and jugular veins. The tubes were inserted subcutaneously and protruded from the neck skin. The mice were allowed to recover for 3–5 days and tubes were flushed with heparinized saline daily[55].

The mice were fasted for 4 h and experiments were initiated in a free-moving condition. After measuring initial blood glucose levels (t = −15 and 0 min), a bolus of insulin (2.5 mU/kg) was injected through the jugular vein and insulin was continuously infused (1 mU/kg/min). Blood glucose levels were measured from arterial blood or tail vein every 5–10 min. Infusion of 30% glucose was performed at a variable rate via the jugular vein catheter to maintain a blood glucose level at 50 mg/dL. Erythrocytes in withdrawn blood were suspended in sterile saline and returned to each animal. After collecting the blood sample at t = 120 min, the mice were anesthetized with isoflurane, and blood samples were collected from the heart to measure CRR hormones. Ice-cold heparinized-saline and subsequent 4% PFA was perfused transcardially to measure cFos, Iba1, and GFAP immunohistochemistry (IHC). Ibuprofen (250 μM, 0.2 μL) or vehicle (5% DMSO in PBS) was injected bilaterally into the VMH 15 min before measuring initial blood glucose levels.

Measurement of serum hormones

After performing the clamp, the blood samples were centrifuged for 10 min at 1000 × *g* and maintained at −30°C until hormones were measured. The concentrations of glucagon, corticosterone, epinepheline, and NE were measured with an ELISA kit (Enzo Life Sciences Inc., Farmingdale, NY). All the protocols followed the instructions provided by the kit.

Immunohistochemistry

For cFos IHC in ibuprofen-treated mice, C57BL/6N male mice received saline or ibuprofen (30 mg/kg body weight) *per os* (p.o.) using a gastric probe 30 min before i.p. injection of saline or insulin (0.75 U/kg). The mice were sacrificed using CO_2 asphyxiation and perfused with heparinized saline transcardially at 60 min after i.p. injection. Brain sections (50 μm each) containing both VMH and ARC were collected from the mice after ibuprofen treatment and the clamp experiment. For cFos staining, the floating sections were incubated with rabbit-anti-cFos antibody (1:1000, Cell Signaling Technology,

#2250S, MA) in blocking solution (0.1 M phosphate buffer (PB) containing 4% normal guinea pig serum, 0.1% glycine, and 0.2% Triton X-100) overnight at room temperature. After rinsing with PB, the sections were incubated in a secondary antibody (1:500, Alexa 488 secondary antibody, Invitrogen, A11008, MA) for 2 h at room temperature.

To assess the hypothalamus inflammation by the population of astrocytes and microglia, sections were treated with 1% H_2O_2 for 15 min followed by incubation with rabbit-anti-Iba1 antibody (1:1000, FUJIFILM Wako Pure Chemical Corporation, 019-19741) or rabbit-anti-GFAP antibody (1:3000, Sigma-Aldrich, HPA056030) in blocking solution overnight at room temperature. After rinsing with PB, sections were incubated in biotinylated goat anti-rabbit (IgG) secondary antibody (1:500, Vector Laboratories, BA1000, Newark, CA) for 1 h at room temperature. The sections were then treated with avidin-biotin complex (ABC) solution (Vector Laboratories) and incubated in 3,3'-diaminobenzidine (DAB) substrate (FUJIFILM Wako Pure Chemical Corporation) for 20 min for Iba1 and 30 min for GFAP after rinsing with PB. The stained sections were washed with PB 3 times and mounted on glass slides with DAPI Fluoromount-G (Southern Biotech, Birmingham, AL). Cells were automatically counted using an ImageJ software plugin (Analyze Particles) or manually counted.

Statistical analysis

Two-way ANOVA and *t*-test were used to determine the effect of insulin, STZ, 2DG, and ibuprofen with the Prism 10 software (GraphPad Software, San Diego, CA). For repeated-measures analysis, two-way ANOVA was used when values over different times were analyzed, followed by the Sidak multiple comparisons tests. For the statistical analysis between four groups, one-way ANOVA was used followed by Tukey's multiple comparisons test. When only two groups were analyzed, statistical significance was determined by the unpaired Student's *t*-test (two-tailed *p*-value). A value of $p < 0.05$ was considered statistically significant. All data are shown as mean ± SEM.

Acknowledgments

We thank Nur Farehan Asgar, PhD, for editing a draft of this manuscript. This work was supported by JSPS KAKENHI (Grant Number 21H02352, 21K18275T, 23H00512); Japan Agency for Medical Research and Development (AMED-RPIME, Grant Number JP21gm6510009h0001,

JP22gm6510009h9901, 23gm6510009h9903, 24gm6510009h9904); the Takeda Science Foundation; the Uehara Memorial Foundation; Astellas Foundation for Research on Metabolic Disorders; Suzuken Memorial Foundation, Akiyama Life Science Foundation, Narishige Neuroscience Research Foundation, and Daiichi Sankyo Foundation of Life Science.

Author contributions

C.T. conceived this study, designed the experiments, and supervised the entire study. T.A. and S. X. performed most of the experiments and analysis. Y.S. performed LC-MS measurements. C.T. and T.H. performed imaging mass spectrometry. T.A, T.I. and Y.A. performed 2DGTT and hypoglycemic clamp. Y.A. measured metabolomics. T.A., S.X., C.T. wrote the manuscript. N.I. and S.D. assisted in preparing the manuscript.

Competing interests

The authors declare that they have no relationships or activities that might bias their work or be perceived as biased.

Legends for figures

Fig. 1 Insulin injection decreases phospholipids in the VMH.

a, A schematic showing the ventromedial (VMH) and arcuate (ARC) nucleus of the hypothalamus. **b**, Representative results of imaging mass spectrometry (IMS) showing the distribution of hypothalamic phosphatidylinositol (PI) (16:0/20:4), PI (18:0/20:4), and PI (18:1/20:4), in mice after injection with saline (left) or insulin (right). The white line shows the position of the VMH and ARC. Scale bar: 200 μm. **c-h,** Relative intensities of PI (c, f), phosphatidylethanolamine (PE) (d, g), and phosphatidylserine (PS) (e, h) in the VMH and ARC 30 min after the saline (n = 5) or insulin (n = 5) i.p. injection. **i, j,** Enzymatic activity of cytosolic PLA2 (i) and secretory PLA2 (j) in the hypothalamus 30 min after the saline (n = 5) or insulin (n = 4) i.p. injection. All results were shown as mean ± SEM, $*p < 0.05$, $**p < 0.01$, $****p < 0.0001$. Two-way ANOVA followed by Sidak multiple comparison tests were used for statistical analysis.

Fig. 2 Glucose deprivation, but not insulin deficiency, changes phospholipids in the hypothalamus.

a-f, Relative intensities of phospholipids in the VMH (a-c) and ARC (d-f) 4 days after i.p. injection with saline (n = 4) or STZ (n = 5). **g-l,** Relative intensities of phospholipids in the VMH (g-i) and ARC (j-l) 60 min after i.p. injection with saline (n = 4) or 2DG (n = 3). All results were shown as mean ± SEM, $*p < 0.05$. One-way ANOVA followed by Tukey's multiple comparison tests were used for statistical analysis.

Fig. 3 Insulin increases prostaglandins in the hypothalamus.

a, Relative amounts of hypothalamic prostaglandins mediated by cyclooxygenase showing mean fold-change in color. **b-f**, Fold-change of 6-keto-PGF1α (b), 11-β-13,14-dihydro-15-keto-PGF2α (c), PGF2α (d), PGF2 (e), and 20-hydroxy-PGF2α (f). All results were shown as mean ± SEM, $*p < 0.05$; $**p < 0.01$. The unpaired Student's *t*-test (two-tailed *p*-value) was used for statistical analysis.

Fig. 4 Central ibuprofen injection impairs glucose production in 2DG-induced glucose deprivation and hypoglycemic clamp.

a, 2DG-induced hyperglycemia in mice that received ibuprofen or vehicle injection (i.c.v.). **b**, Area under the curve of blood glucose in (a). **c**, Food intake after i.p. injection of 2DG in ibuprofen or vehicle-injected mice (i.c.v.). **d,** Blood glucose levels during hyperinsulinemic-hypoglycemic clamp in mice that received ibuprofen or vehicle injection into the VMH bilaterally. Insulin infusion was started at t = 0 min. **e**, Glucose infusion rate to maintain hypoglycemia at 50 mg/dL during clamp. **f-i**, Concentration of serum hormones, glucagon (f), corticosterone (g), epinephrine (h), and norepinephrine (i), corrected at 120 min of the clamp experiment. All results were shown as mean ± SEM, *$p < 0.05$; **$p < 0.01$; ***$p < 0.001$; ****$p < 0.0001$. The unpaired Student's *t*-test (two-tailed *p*-value) and two-way ANOVA followed by Sidak multiple comparison tests were used for statistical analysis.

Fig. 5 Ibuprofen decreased insulin-induced cFos-positive cells specifically in ventrolateral VMH.

a, Representative micrographs of cFos immunoreactivity in the VMH and ARC. Scale bar: 100 µm. White lines indicate the boundary of the nucleus in the hypothalamus. **b-c,** Quantification of cFos cell number in dorsomedial (dm), central (c) and ventrolateral (vl) part of the VMH (b) and arcuate nucleus (ARC) (c) in the mice that received vehicle (po) and vehicle (ip) (vehi+vehi), ibuprofen (po) and vehicle (ip) (ibu+vehi), vehicle (po) and insulin (ip) (vehi+ins), ibuprofen (po) and insulin (ip) (ibu+ins). All results were shown as mean ± SEM, *$p < 0.05$; **$p < 0.01$. One-way ANOVA followed by Tukey's multiple comparison tests were used for statistical analysis.

Fig. 6 Recurrent hypoglycemia decreases glucose production and shows metabolic adaptation in the hypothalamus

a, Daily blood glucose levels during 5 days of recurrent hypoglycemia. **b**, Blood glucose levels during hypoglycemic clamp. Insulin infusion was started at t = 0 min. **c**, Glucose infusion rate to maintain hypoglycemia at 50 mg/dL during clamp and average GIR in the last 40 min. **d-g**, The relative amount of glycolytic intermediates (a) TCA cycle intermediates (b), amino acids (c) and neurotransmitters (g) in the hypothalamus 30 min after insulin (1 U/kg) or saline injection in control mice. Data is shown as arbitrary unit (AU). **h-k**, The relative amount of glycolytic intermediates (h)

TCA cycle intermediates (i), amino acids (j), and neurotransmitters (k) in the hypothalamus 30 min after insulin (1 U/kg) or saline injection in RH-treated mice. All results were shown as mean ± SEM, *$p < 0.05$; **$p < 0.01$; ***$p < 0.001$; ****$p < 0.0001$. The unpaired Student's *t*-test (two-tailed *p*-value) and two-way ANOVA followed by Sidak multiple comparison tests were used for statistical analysis.

Fig. 7 shRNA against cPLA2 in the hypothalamus improves RH-induced impairment of glucose production

a, A schematic illustrating AAV injection into the VMH. **b**, Representative image of RFP expression after AAV injection. **c**, mRNA expression of cPLA2 in the hypothalamus. **d**, Experimental timeline of AAV injection, RH, and hypoglycemic clamp. **e**, Daily blood glucose levels during 5 days of recurrent hypoglycemia. **f**, Blood glucose levels during hypoglycemic clamp. Insulin infusion was started at t = 0 min. **g**, Glucose infusion rate to maintain hypoglycemia at 50 mg/dL during clamp and average GIR in the last 40 min. **h-k**, Concentration of serum hormones, glucagon (h), corticosterone (i), epinephrine (j), and norepinephrine (k), corrected at 120 min of the clamp experiment. **l-o**, numbers of Iba1 (l), GFAP (m) and cFos-positive cells (n, o) per section in the whole VMH and ventrolateral part of the VMH. All results were shown as mean ± SEM, *$p < 0.05$; **$p < 0.01$; ***$p < 0.001$; ****$p < 0.0001$. The unpaired Student's *t*-test (two-tailed *p*-value) and two-way ANOVA followed by Sidak multiple comparison tests were used for statistical analysis.

Graphical Abstract

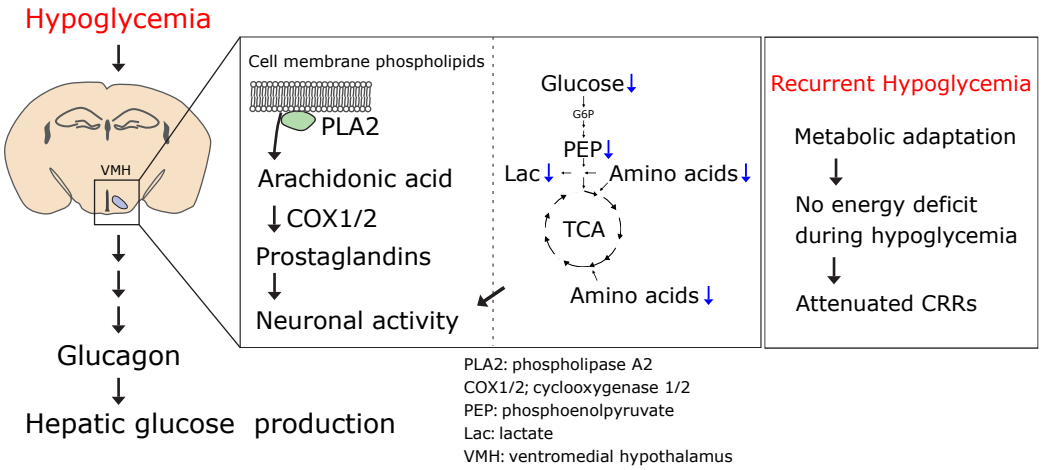

PLA2: phospholipase A2
COX1/2; cyclooxygenase 1/2
PEP: phosphoenolpyruvate
Lac: lactate
VMH: ventromedial hypothalamus

Fig. 1

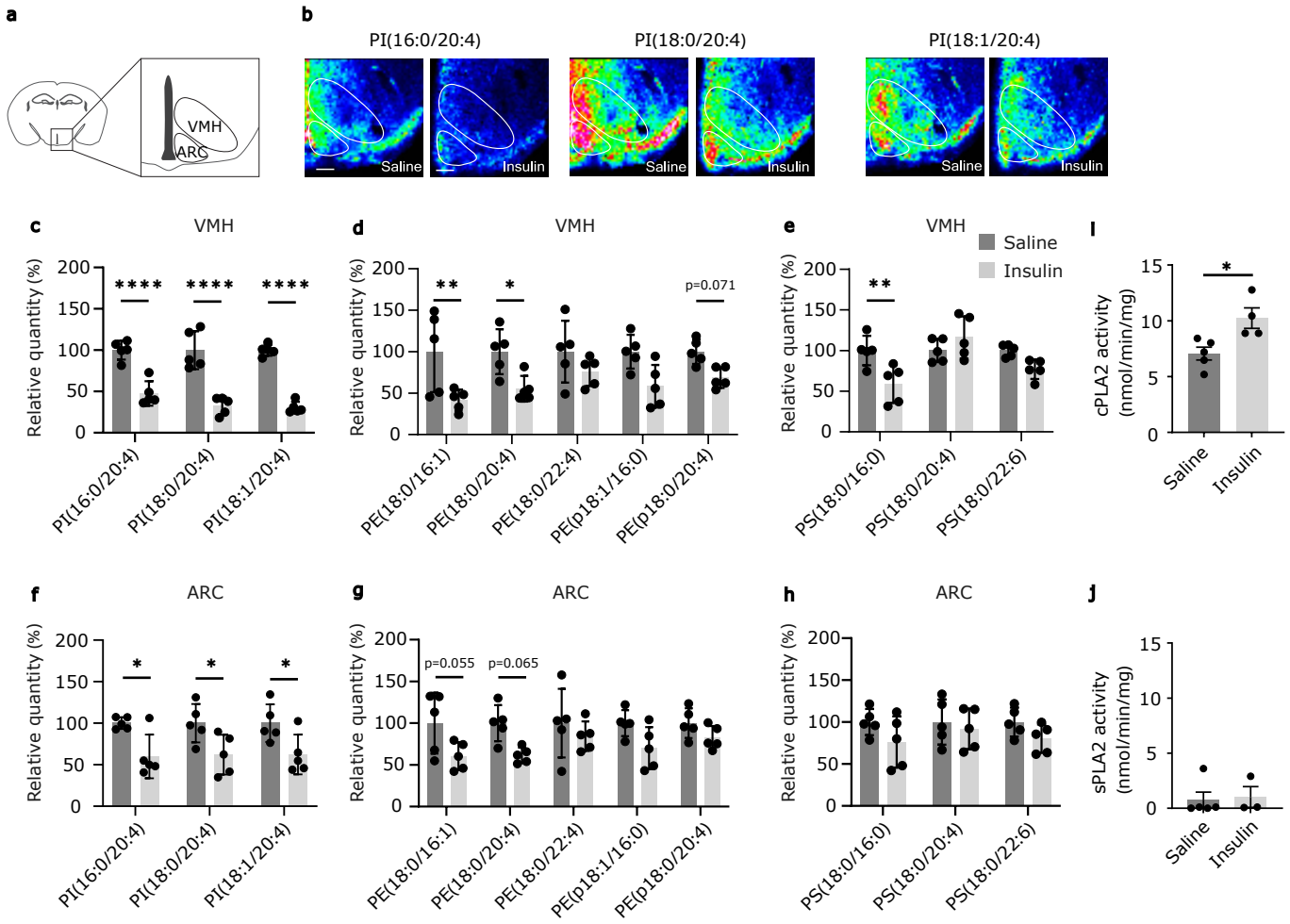

Fig. 1 Insulin injection decreases phospholipids in the VMH.

a, A schematic showing the ventromedial (VMH) and arcuate (ARC) nucleus of the hypothalamus. **b,** Representative results of imaging mass spectrometry (IMS) showing the distribution of hypothalamic phosphatidylinositol (PI) (16:0/20:4), PI (18:0/20:4), and PI (18:1/20:4), in mice after injection with saline (left) or insulin (right). The white line shows the position of the VMH and ARC. Scale bar: 200 μm. **c-h,** Relative intensities of PI (c, f), phosphatidylethanolamine (PE) (d, g), and phosphatidylserine (PS) (e, h) in the VMH and ARC 30 min after the saline (n = 5) or insulin (n = 5) i.p. injection. **i, j,** Enzymatic activity of cytosolic PLA2 (i) and secretory PLA2 (j) in the hypothalamus 30 min after the saline (n = 5) or insulin (n = 4) i.p. injection. All results were shown as mean ± SEM, *$p < 0.05$, **$p < 0.01$, ****$p < 0.0001$. Two-way ANOVA followed by Sidak multiple comparison tests were used for statistical analysis.

Fig. 2

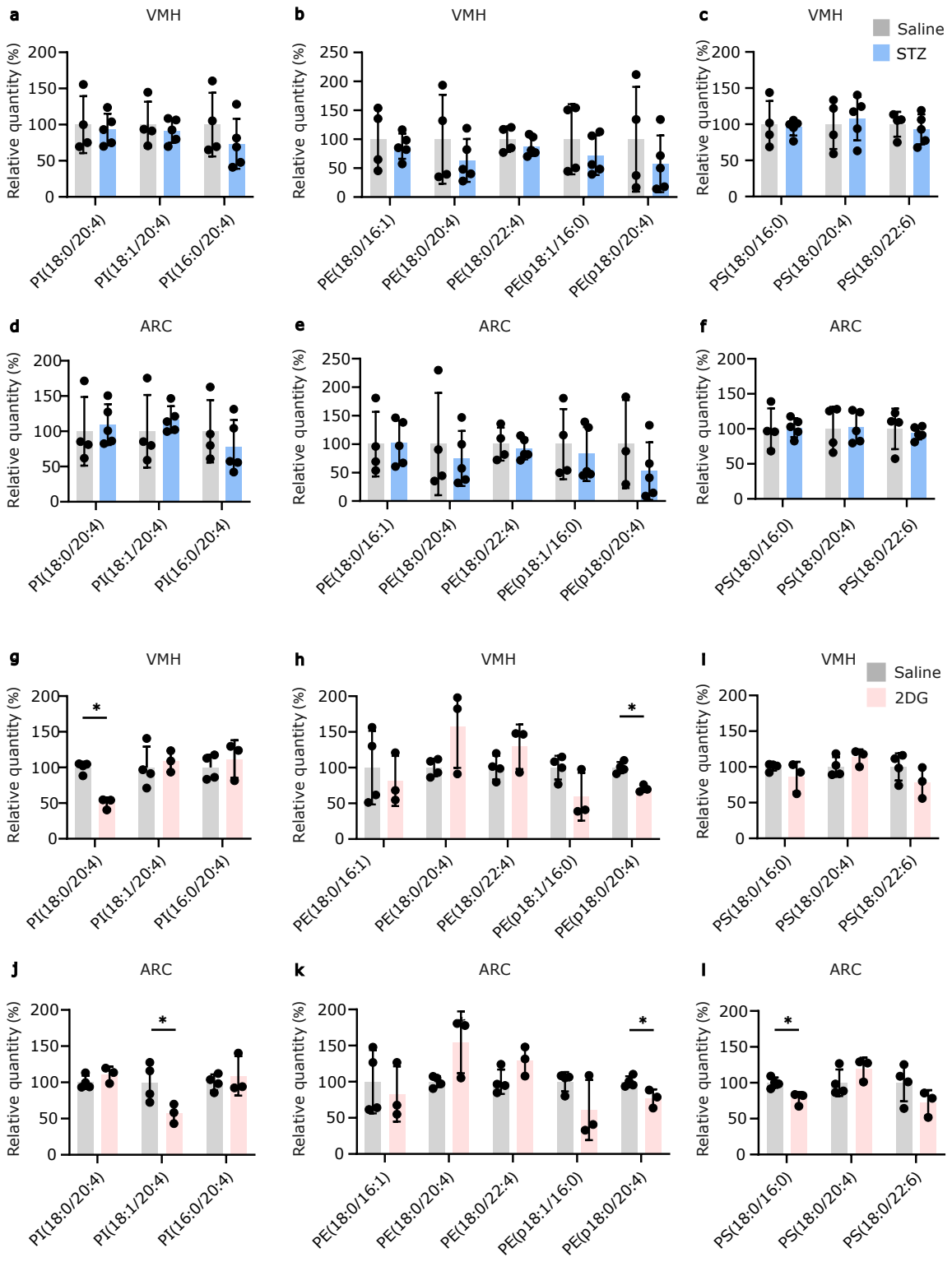

Fig. 2 Glucose deprivation, but not insulin deficiency, changes phospholipids in the hypothalamus.
a-f, Relative intensities of phospholipids in the VMH (a-c) and ARC (d-f) 4 days after i.p. injection with saline (n = 4) or STZ (n = 5). **g-l**, Relative intensities of phospholipids in the VMH (g-i) and ARC (j-l) 60 min after i.p. injection with saline (n = 4) or 2DG (n = 3). All results were shown as mean ± SEM, *$p < 0.05$. One-way ANOVA followed by Tukey's multiple comparison tests were used for statistical analysis.

Fig. 3

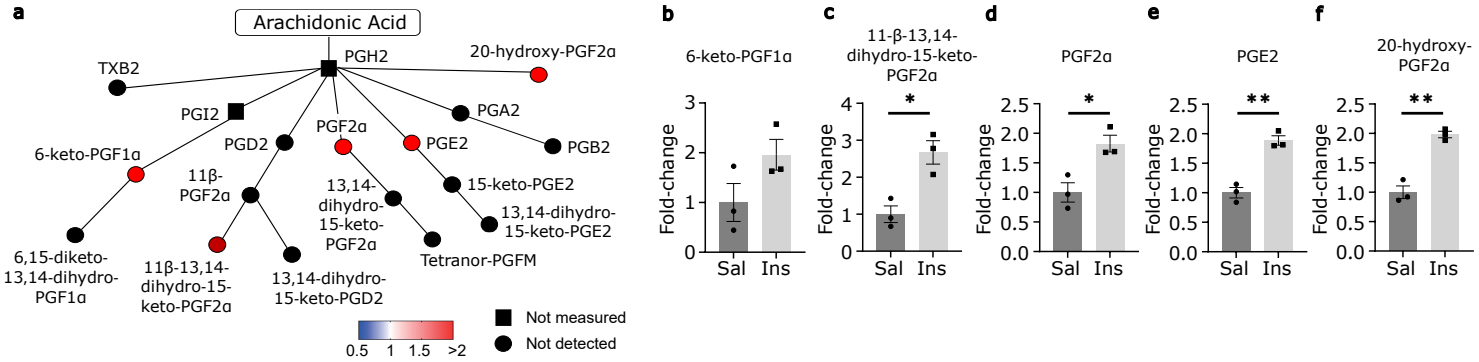

Fig. 3 Insulin increases prostaglandins in the hypothalamus.

a, Relative amounts of hypothalamic prostaglandins mediated by cyclooxygenase showing mean fold-change in color. **b-f,** Fold-change of 6-keto-PGF1α (b), 11-β-13,14-dihydro-15-keto-PGF2α (c), PGF2α (d), PGF2 (e), and 20-hydroxy-PGF2α (f). All results were shown as mean ± SEM, *$p < 0.05$; **$p < 0.01$. The unpaired Student's t-test (two-tailed p-value) was used for statistical analysis.

Fig. 4

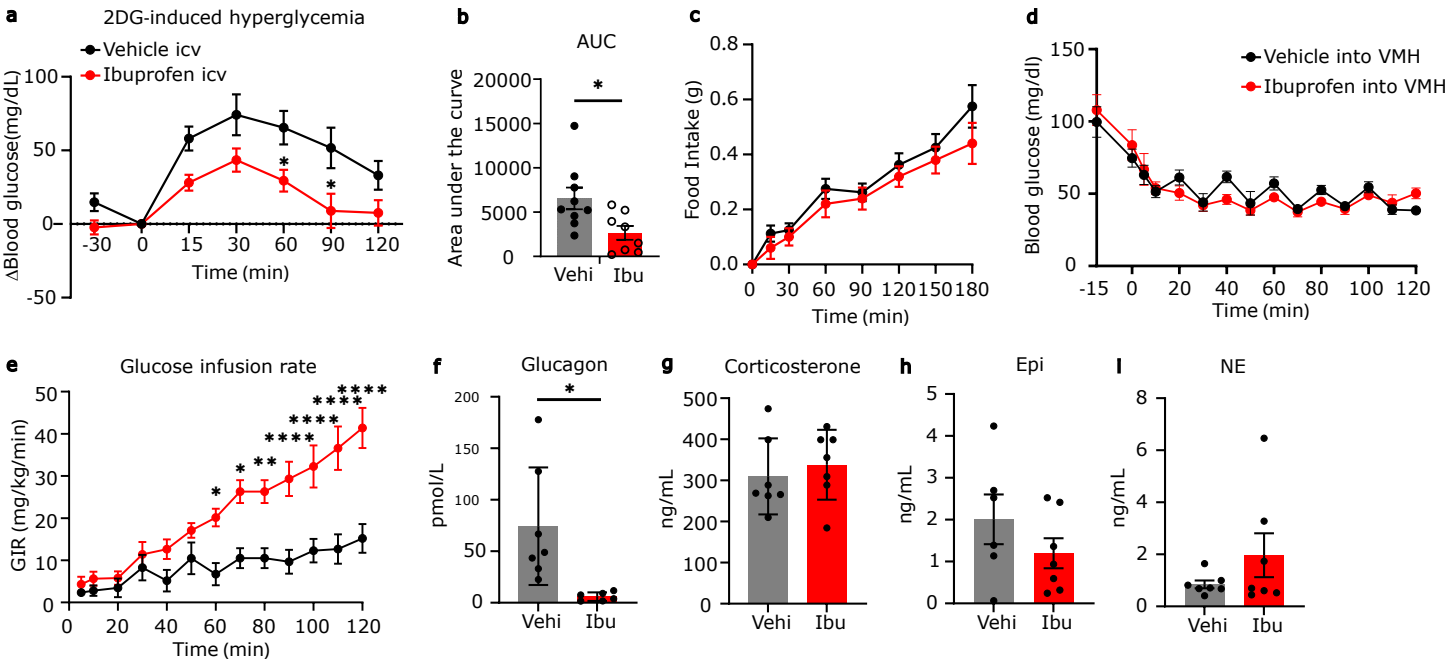

Fig. 4 Central ibuprofen injection impairs glucose production in 2DG-induced glucose deprivation and hypoglycemic clamp.

a, 2DG-induced hyperglycemia in mice that received ibuprofen or vehicle injection (i.c.v.). **b,** Area under the curve of blood glucose in (a). **c**, Food intake after i.p. injection of 2DG in ibuprofen or vehicle-injected mice (i.c.v.). **d**, Blood glucose levels during hyperinsulinemic-hypoglycemic clamp in mice that received ibuprofen or vehicle injection into the VMH bilaterally. Insulin infusion was started at t = 0 min. **e**, Glucose infusion rate to maintain hypoglycemia at 50 mg/dL during clamp. **f-i,** Concentration of serum hormones, glucagon (f), corticosterone (g), epinephrine (h), and norepinephrine (i), corrected at 120 min of the clamp experiment. All results were shown as mean ± SEM, *p < 0.05; **p < 0.01; ***p < 0.001; ****p < 0.0001. The unpaired Student's t-test (two-tailed p-value) and two-way ANOVA followed by Sidak multiple comparison tests were used for statistical analysis.

Fig. 5

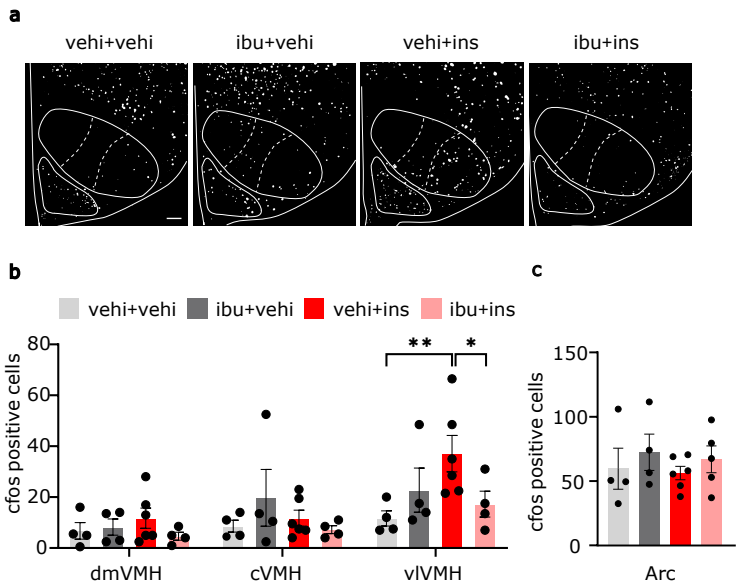

Fig. 5 Ibuprofen decreased insulin-induced cFos-positive cells specifically in ventrolateral VMH.
a, Representative micrographs of cFos immunoreactivity in the VMH and ARC. Scale bar: 100 μm. White lines indicate the boundary of the nucleus in the hypothalamus. **b-c**, Quantification of cFos cell number in dorsomedial (dm), central (c) and ventrolateral (vl) part of the VMH (b) and arcuate nucleus (ARC) (c) in the mice that received vehicle (po) and vehicle (ip) (vehi+vehi), ibuprofen (po) and vehicle (ip) (ibu+vehi), vehicle (po) and insulin (ip) (vehi+ins), ibuprofen (po) and insulin (ip) (ibu+ins). All results were shown as mean ± SEM, *$p < 0.05$; **$p < 0.01$. One-way ANOVA followed by Tukey's multiple comparison tests were used for statistical analysis.

Fig. 6

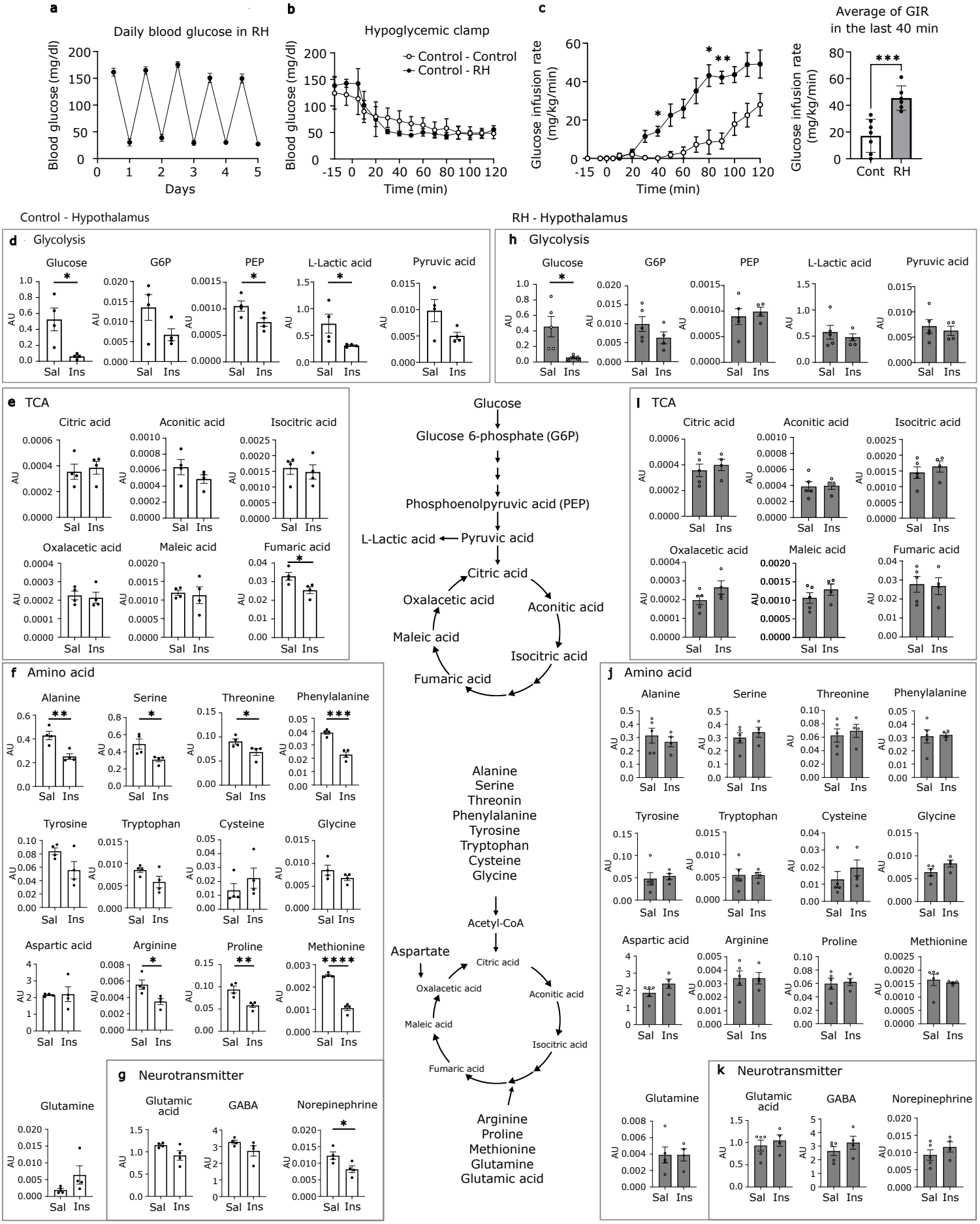

Fig. 6 Recurrent hypoglycemia decreases glucose production and shows metabolic adaptation in the hypothalamus

a, Daily blood glucose levels during 5 days of recurrent hypoglycemia. **b,** Blood glucose levels during hypoglycemic clamp. Insulin infusion was started at t = 0 min. **c,** Glucose infusion rate to maintain hypoglycemia at 50 mg/dL during clamp and average GIR in the last 40 min. **d-g,** The relative amount of glycolytic intermediates (a) TCA cycle intermediates (b), amino acids (c) and neurotransmitters (g) in the hypothalamus 30 min after insulin (1 U/kg) or saline injection in control mice. Data is shown as arbitrary unit (AU). **h-k,** The relative amount of glycolytic intermediates (h) TCA cycle intermediates (i), amino acids (j), and neurotransmitters (k) in the hypothalamus 30 min after insulin (1 U/kg) or saline injection in RH-treated mice. All results were shown as mean ± SEM, *p < 0.05; **p < 0.01; ***p < 0.001; ****p < 0.0001. The unpaired Student's t-test (two-tailed p-value) and two-way ANOVA followed by Sidak multiple comparison tests were used for statistical analysis.

Fig. 7

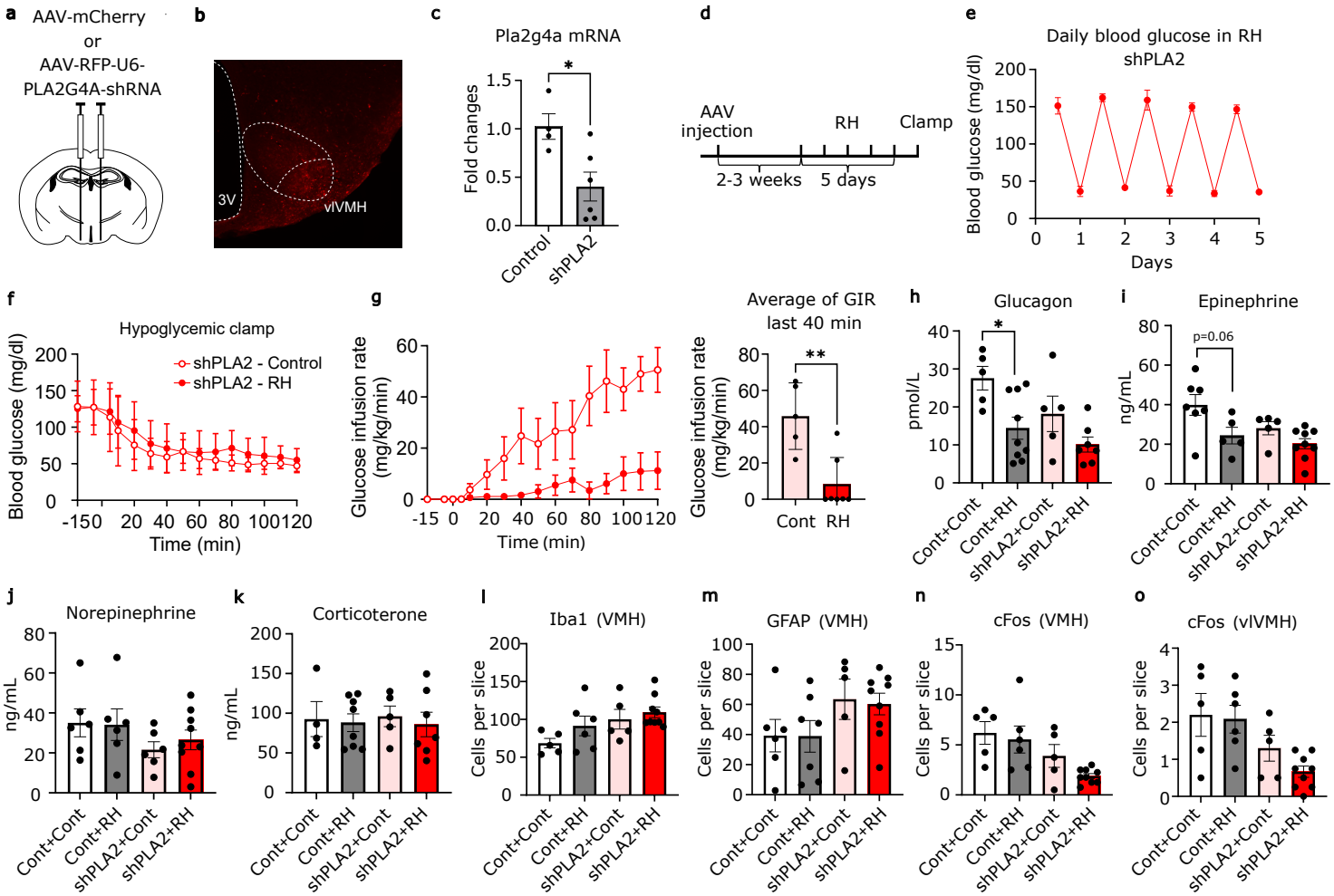

Fig. 7 shRNA against cPLA2 in the hypothalamus improves RH-induced impairment of glucose production

a, A schematic illustrating AAV injection into the VMH. **b,** Representative image of RFP expression after AAV injection. **c**, mRNA expression of cPLA2 in the hypothalamus. **d,** Experimental timeline of AAV injection, RH, and hypoglycemic clamp. **e,** Daily blood glucose levels during 5 days of recurrent hypoglycemia. **f,** Blood glucose levels during hypoglycemic clamp. Insulin infusion was started at t = 0 min. **g,** Glucose infusion rate to maintain hypoglycemia at 50 mg/dL during clamp and average GIR in the last 40 min. **h-k,** Concentration of serum hormones, glucagon (h), corticosterone (i), epinephrine (j), and norepinephrine (k), corrected at 120 min of the clamp experiment. **l-o,** numbers of Iba1 (l), GFAP (m) and cFos-positive cells (n, o) per section in the whole VMH and ventrolateral part of the VMH. All results were shown as mean ± SEM, *p < 0.05; **p < 0.01; ***p < 0.001; ****p < 0.0001. The unpaired Student's t-test (two-tailed p-value) and two-way ANOVA followed by Sidak multiple comparison tests were used for statistical analysis.

Table S1

Blood glucose at sacrifice in each figure

Treatment	mg/dL
Fig. 1	
Saline	133.2 ± 2.3
Insulin	71.6 ± 6.5
Fig. 2	
Saline	129.8 ± 6.9
STZ	442.8 ± 35.5
Saline	129.3 ± 5.6
2DG	197.3 ± 20.8
Fig. 3	
Saline	127.0 ± 5.3
Insulin	46.7 ± 9.8
Fig. 6 Metabolomics	
Cont - Saline	178.8 ± 12.0
Cont - Insulin	36.3 ± 8.4
RH - Saline	151.2 ± 10.4
RH - Insulin	37.3 ± 3.6

Mouse qPCR Primer sequences

Pla2g4a	Forward	GATGAGGCTCAAGGACCCAAAG
	Reverse	GAATAAAGCCGAGTCGCTCACC
Actin beta (ActB)	Forward	CATTGCTGACAGGATGCAGAAGG
	Reverse	TGCTGGAAGGTGGACAGTGAGG